

Discovery and Engineering of the Cocaine Biosynthetic Pathway

Yong-Jiang Wang,[#] Jian-Ping Huang,[#] Tian Tian,[#] Yijun Yan, Yin Chen, Jing Yang, Jianghua Chen, Yu-Cheng Gu, and Sheng-Xiong Huang*



Cite This: <https://doi.org/10.1021/jacs.2c09091>



Read Online

ACCESS |



Metrics & More

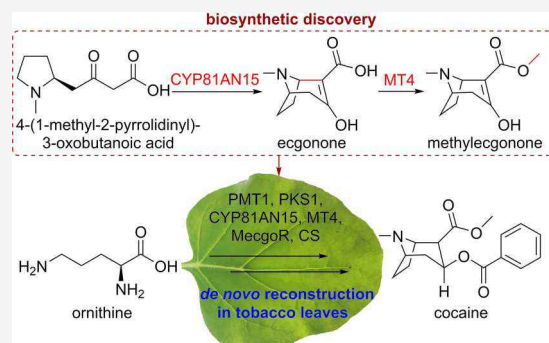


Article Recommendations



Supporting Information

ABSTRACT: Cocaine, the archetypal tropane alkaloid from the plant genus *Erythroxylum*, has recently been used clinically as a topical anesthesia of the mucous membranes. Despite this, the key biosynthetic step of the requisite tropane skeleton (methylecgonone) from the identified intermediate 4-(1-methyl-2-pyrrolidinyl)-3-oxobutanoic acid (MPOA) has remained, until this point, unknown. Herein, we identify two missing enzymes (*EnCYP81AN15* and *EnMT4*) necessary for the biosynthesis of the tropane skeleton in cocaine by transient expression of the candidate genes in *Nicotiana benthamiana*. Cytochrome P450 *EnCYP81AN15* was observed to selectively mediate the oxidative cyclization of S-MPOA to yield the unstable intermediate ecgonone, which was then methylated to form optically active methylecgonone by methyltransferase *EnMT4* in *Erythroxylum novogranatense*. The establishment of this pathway corrects the long-standing (but incorrect) biosynthetic hypothesis of MPOA methylation first and oxidative cyclization second. Notably, the de novo reconstruction of cocaine was realized in *N. benthamiana* with the two newly identified genes, as well as four already known ones. This study not only reports a near-complete biosynthetic pathway of cocaine and provides new insights into the metabolic networks of tropane alkaloids (cocaine and hyoscyamine) in plants but also enables the heterologous synthesis of tropane alkaloids in other (micro)organisms, entailing significant implications for pharmaceutical production.



INTRODUCTION

Being principally produced by the Erythroxylaceae family of plants, cocaine and its derivatives have been utilized by humans for thousands of years. Indeed, indigenous South Americans were known to chew coca leaves to provide nutrition and elevate the spirit.¹ In the 19th century, cocaine was used as effective local anesthesia for eye surgery, solving the dilemma of ocular surgery without anesthetics.² Subsequently, cocaine gradually became the active ingredient in many drugs developed to treat a variety of diseases and was even the active component in well-known beverages.² The ensuing popularity and consequential addiction of cocaine resulted in its prohibition outside of pharmaceutical use. Recently, cocaine (Goprelto and Numbrino) has been approved by the FDA for use as a topical anesthesia of mucous membranes due to its advantageous stability and vasoconstrictive properties.

Cocaine (1) and hyoscyamine (2), the most commonly known tropane alkaloids, are structurally distinct at the C-2 and C-3 positions (Figure 1), which are key to their affinity for dopamine receptors and contribute to their unique euphoric properties.³ Even after more than 100 years of investigation, the biosynthetic route of cocaine (1) still remains incomplete, though the route toward hyoscyamine (2) has recently been fully clarified.^{4–6} Previous isotopic labeling experiments^{7,8} have suggested that cocaine (1) and

hyoscyamine (2) share a common precursor, namely, 4-(1-methyl-2-pyrrolidinyl)-3-oxobutanoic acid (MPOA, 3) (Figure 1).^{9,10} The identification of the precursor methyl 4-(1-methyl-2-pyrrolidinyl)-3-oxobutanoate (MMPO, 4, which was suggested by in vivo labeling studies⁷) has led to the hypothesis that the central tropane ring in cocaine (1) is derived from 4.^{9,10} Notably, this proposal implies the existence of a methyltransferase which, despite considerable exploration, has not been identified. After methylation, 4 would then undergo oxidative cyclization to form methylecgonone (5) in a similar manner to the biosynthesis of hyoscyamine (2) (Figure 1).¹¹ In this study, however, we report the identification and characterization of the enzymes responsible for an unexpected biosynthesis of methylecgonone (5), and so also cocaine (1), in *E. novogranatense*.

Received: August 25, 2022

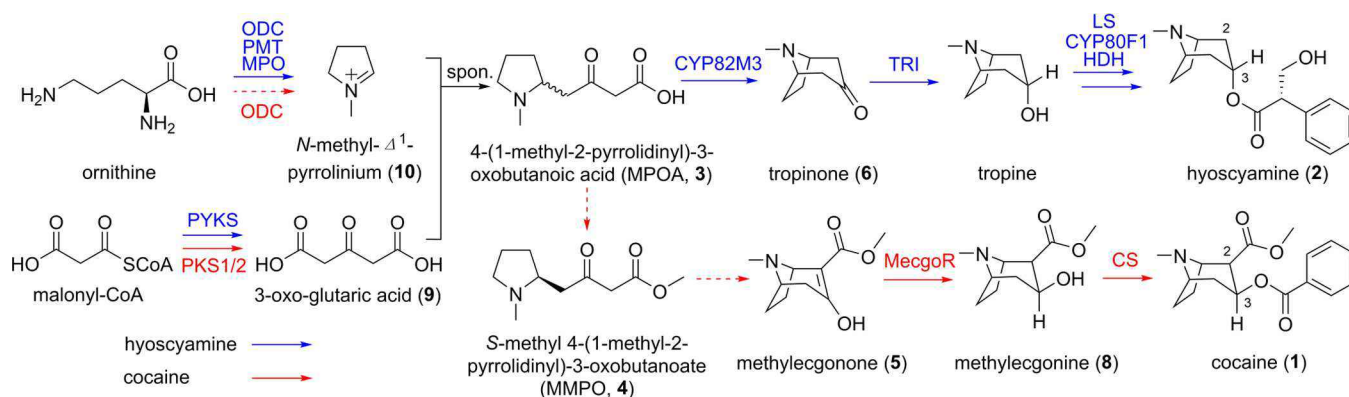


Figure 1. Proposed biosynthetic routes of cocaine and hyoscyamine.^{6,9,10} Uncharacterized steps are indicated by dashed lines. ODC: ornithine decarboxylase; PMT: putrescine *N*-methyltransferase; MPO: *N*-methylputrescine oxidase; PKS: polyketide synthase; PYKS: pyrrolidine ketide synthase; MecgoR: methylecgonone reductase; CS: cocaine synthase; CYP82M3: tropinone synthase; TRI: tropinone reductase I; LS: littorine synthase; CYP80F1: littorine mutase; HDH: hyoscyamine dehydrogenase.

RESULTS

Attempts to Discover MPOA Methyltransferase and MMPO Oxidase in *E. novogranatense* Were Not Successful.

To explore the biosynthesis of the tropane skeleton in cocaine (1), we first focused on the methylation of 3 as isotopic labeling experiments indicated that 4 was incorporated into 1 (Figure 1).⁷ Since all previously characterized enzymes for the methylation of carboxylic acid groups in plants belong to the SABATH (salicylic acid/benzoic acid/theobromine) methyltransferase family,^{12,13} we located 23 SABATH methyltransferase genes in the transcriptome of *E. novogranatense* by an HMM (hidden Markov model) search. Based on the tissue-specific expression of cocaine biosynthetic genes in buds and young leaves (Figure S1),^{14–16} six candidate genes (*EnMT1–5* and *EnMT9*), exhibiting expression in these tissues [fragments per kilo base of transcript per million mapped fragments (FPKM) > 5.0], were cloned from *E. novogranatense* cDNA and transiently expressed in *Nicotiana benthamiana* leaves mediated by *Agrobacterium tumefaciens* LBA4404. As a result, the transient expression of *EnMT2* or *EnMT4* proteins led to the formation of trace 4 when supplemented with substrate 3 (Figure S2). Subsequently, these two proteins were heterologously expressed in *Escherichia coli* and tested for reactivity with 3 in vitro. As before, only a small amount of methylated product 4 could be detected by liquid chromatography mass spectrometry (LC–MS) analysis (Figure S3). The low amount of product turnover from these assays suggested that 3 was not the native substrate for either *EnMT2* or *EnMT4*, leading us to question their exact catalytic function.

At the same time, we pursued the identity of the oxidase enzyme responsible for the ring closure of 4 in *E. novogranatense* (Figure 1). Given that this process is similar to that for the formation of tropinone (6, catalyzed by CYP82M3 in Solanaceae¹¹), we first verified the functions of CYP82 family genes in *E. novogranatense*. Seven CYP82 family candidate genes (*EnCYP1–7*, FPKM > 5.0 in bud and young leaf, Figure S4) were expressed in *N. benthamiana* or *Saccharomyces cerevisiae*. With the supplement of substrate 4, no methylecgonone (5) was detected, which strongly suggests that the oxidative cyclization of 4 is not catalyzed by CYP82 enzymes in *E. novogranatense*. Subsequently, all cytochrome P450 (CYP450), flavin-dependent monooxygenase (FAD), and 2-oxoglutarate-dependent dioxygenase (ODG) genes in

the transcriptome of *E. novogranatense* were screened by tissue-specific expression analysis. The obtained candidate genes (nine CYP450 genes, two FAD genes, and three ODG genes, Figure S5), which showed similar tissue expression pattern with functional characterized genes involved in cocaine biosynthesis, were tested in *N. benthamiana* or *S. cerevisiae*, though no product 5 could be detected.

Biosynthetic Route of the Tropane Skeleton in *E. novogranatense*. The failure to discover the biosynthetic genes responsible for the formation of 4 and 5 from 3 and 4, respectively (i.e., methylation and then oxidative cyclization) led us to reassess the order of the prevailing biosynthetic hypothesis. As such, we speculated that formation of the tropane ring in 5 likely occurred before methylation of the carboxylic acid (Figure 2a). We reasoned that the most effective way to verify this would be to iteratively co-express candidate oxidases and methyltransferases. In the event, LC–MS analysis revealed that 5 was produced when oxidase *EnCYP81AN15* and methyltransferase *EnMT4* were co-expressed in *N. benthamiana* with supplemented 3 (Figures 2b and S6a). Contrary to our expectations, tropinone (6) was also detected, especially when *EnCYP81AN15* was expressed alone (Figure S6b). In order to systematically characterize the function of the relevant enzymes, *EnCYP81AN15* and *EnMT4* were separately expressed in *S. cerevisiae* and *E. coli* (Figure S7), respectively, and then combined to test their reactivity toward substrate 3 in vitro. As expected, 5 could be detected in the assay when *EnCYP81AN15* and *EnMT4* were co-incubated (Figure 2c). These results provide strong evidence for the actual order of events in methylecgonone (5) biosynthesis (Figure 2a). Namely, 3 (and not 4) is oxidized and cyclized by *EnCYP81AN15* to form the unstable intermediate ecgonone (7), which is then methylated by *EnMT4* to form 5. The side product tropinone (6) is likely formed by the spontaneous decarboxylation of 7.

In order to verify that unstable 7 was indeed the native substrate of *EnMT4*, we sought to obtain 7 by chemical means. Drawing inspiration from Robinson's classical total synthesis of tropinone (6) and methylecgonone (5) (Figure S8),^{17,18} we speculated that ecgonone (7) could also be attained by a cognate route through the use of simple 3-oxoglutaric acid (9), so long as careful handling avoided unwanted decarboxylation. Fortunately, 7 could be obtained (existing mainly as the enol isomer in the aqueous solution) and thus was utilized as the

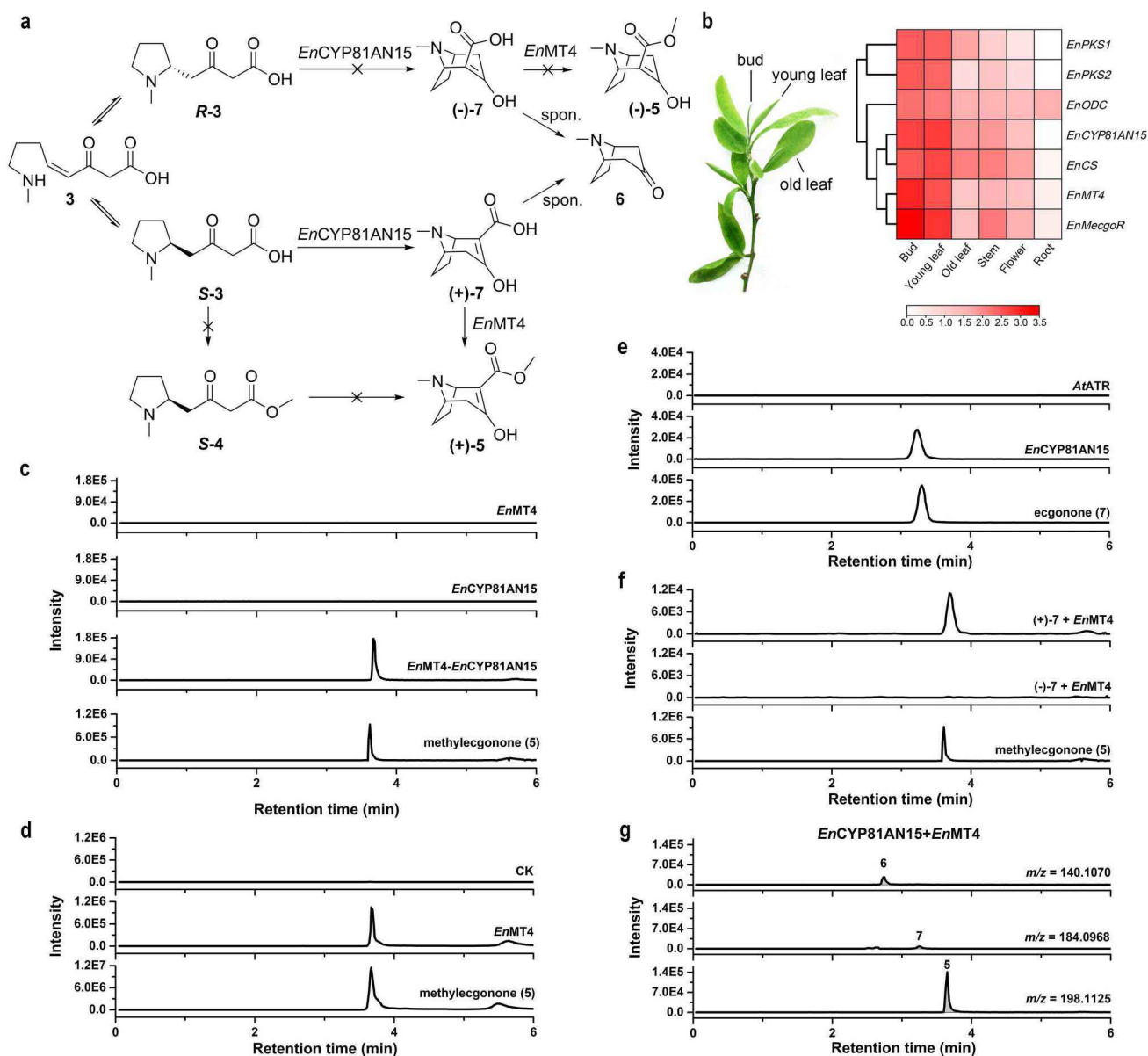


Figure 2. Biosynthesis of the tropane skeleton in cocaine. (a) Proposed biosynthetic routes for the tropane skeleton in cocaine. (b) Expression patterns of *EnCYP81AN15*, *EnMT4*, and functional characterized genes involved in cocaine biosynthesis. *EnCYP81AN15* and *EnMT4* showed the characteristic bud and young leaf-predominant expression pattern. The photo of *E. novogranatense* was taken in the Xishuangbanna tropical botanical garden, China. (c) Extracted ion chromatograms (EICs) for methylecgonone (**5**, $m/z = 198.1125 \pm 0.0010$) catalyzed by *EnMT4* and *EnCYP81AN15* with racemic **3** in vitro. (d) EICs for methylecgonone (**5**, $m/z = 198.1125 \pm 0.0010$) catalyzed by *EnMT4* with racemic **7** in vitro. (e) EICs for ecgonone (**7**, $m/z = 184.0968 \pm 0.0010$) catalyzed by *EnCYP81AN15* and *AtATR1* with racemic **3** in vitro. (f) EICs for methylecgonone (**5**, $m/z = 198.1125 \pm 0.0010$) catalyzed by *EnMT4* with (+)-**7** or (-)-**7** in vitro. (g) EICs for tropinone (**6**), ecgonone (**7**), and methylecgonone (**5**) catalyzed by *EnCYP81AN15* and *EnMT4* with racemic **3** in vitro.

substrate of *EnMT4*. The incubation of **7** with *EnMT4* efficiently gave the methylated product **5** (Figure 2d), thus corroborating its status as the native substrate. At the same time, the incubation of **3** with *EnCYP81AN15* in vitro was verified to yield unstable **7**, suggesting that **7** is the native product of *EnCYP81AN15* (Figure 2e). The spontaneous decarboxylation of **7** over time led to the accumulation of tropinone (**6**) (Figure S9). Notably, CYP82M3 has previously been reported to yield **6** and not **7**.¹¹ In our hands, however, **7** could be detected when CYP82M3 was incubated with **3**, followed by a mild post-reaction procedure (Figure S10). Besides, when *EnMT4* was co-incubated with CYP82M3 not *EnCYP81AN15* in vitro and in *N. benthamiana*, the methylated

product **5** could be detected with supplemented **3** (Figure S11). Thus, *EnCYP81AN15* or CYP82M3 should instead be designated as ecgonone synthases (ESs). These results firmly establish that oxidative cyclization (i.e., formation of a tropane ring) occurs before the methylation of substrate **3** in *E. novogranatense* (Figure 2a).

In hyoscyamine biosynthesis, there is an unresolved question about the enantioselectivity of CYP82M3 for substrate **3**.¹¹ It is possible that racemic **3** is catalyzed by CYP82M3 to form racemic **7**, which undergoes spontaneous decarboxylation to form achiral **6**.¹¹ For cocaine (**1**), the existence of enantiopure intermediate **5**¹⁴ suggests that (+)-**7** should be the product of *EnCYP81AN15* (Figure 2a). If not, (-)-**7** will undergo

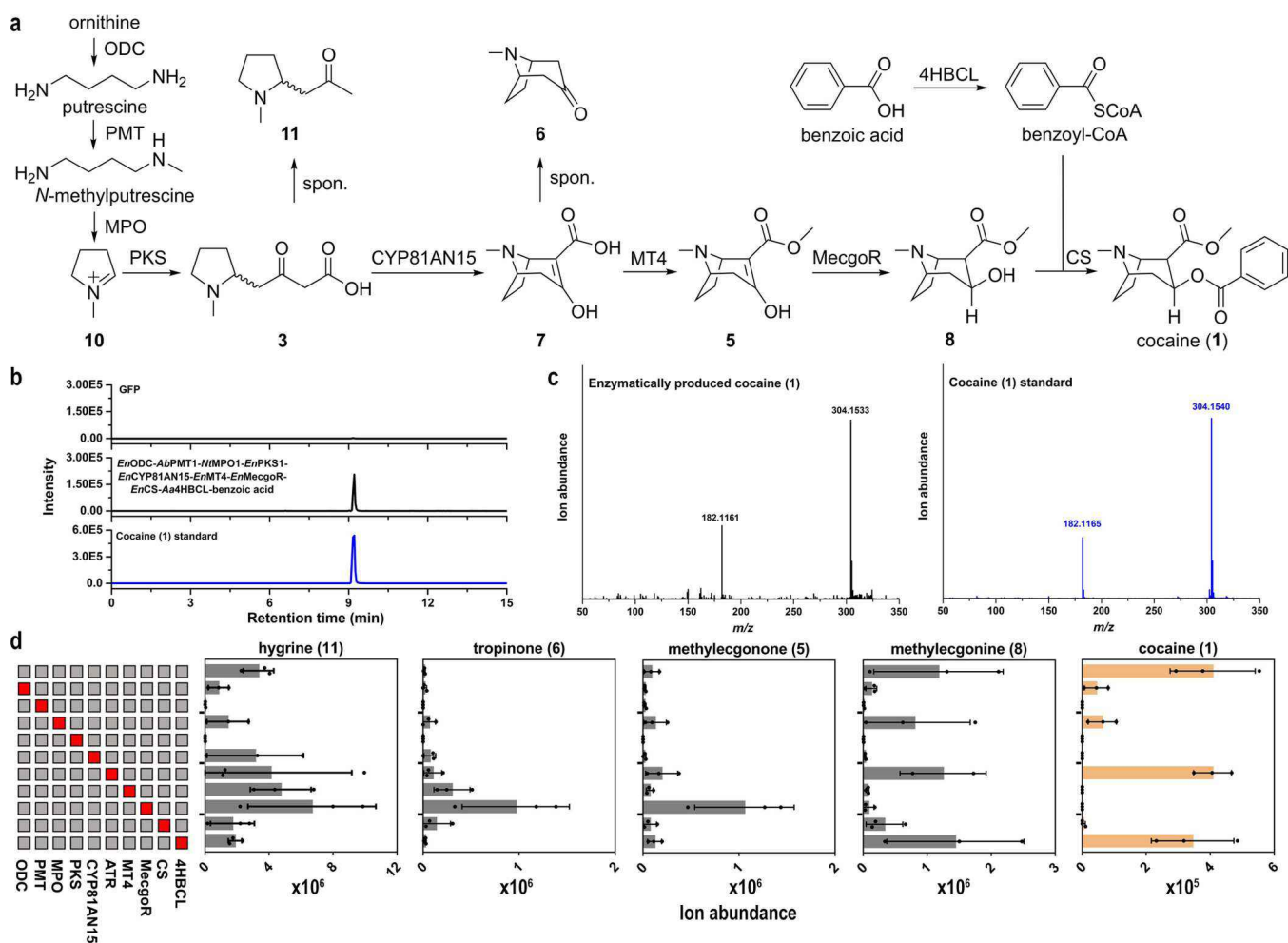


Figure 3. Reconstruction of the cocaine biosynthetic pathway in tobacco. (a) Biosynthetic route of cocaine in tobacco. (b) EIC for cocaine (**1**, $m/z = 304.1543 \pm 0.0010$) produced by transiently expressed enzymes in tobacco leaves, compared to the authentic standard of cocaine (**1**). (c) MS/MS fragmentation of cocaine (**1**) produced by transiently expressed enzymes in tobacco leaves, compared to the fragmentation of cocaine (**1**) standard. (d) Average LC-MS ion abundance \pm standard deviation (SD, three biological replicates) is shown for cocaine intermediates and derivatives produced in tobacco. Red boxes indicate the deleted enzyme.

spontaneous decarboxylation to form **6** or be methylated by *EnMT4* to form (-)-**5**. First, we tested the reactivity of *EnMT4* toward substrate (+)-**7** and (-)-**7**. Indeed, incubation of (+)-ecgonone (**7**) led cleanly to methylecgonone (**5**), while no product was observed with (-)-ecgonone (**7**) (Figure 2a,f), which suggests that *EnMT4* is highly selective for (+)-**7**. Even in the presence of an enantioselective methylation step, it is plausible that **7** is formed as a racemate with unreacted (-)-**7** undergoing spontaneous decarboxylation to form tropinone (**6**) (Figure 2a). Subsequently, we incubated racemic **3** with *EnCYP81AN15* and *EnMT4* in vitro. In this assay, the major product **7** of *EnCYP81AN15* was observed to be **5**, with only a small amount of **6** detected (Figure 2g). These results indicate that *EnCYP81AN15* likely catalyzes S-3 to form (+)-**7** (Figure 2a), with similar behavior observed for CYP82M3 (Figure S12). Thus, both *EnCYP81AN15* and CYP82M3 yield (+)-**7** from S-3 and not (-)-**7** from R-3. Besides, R-3 may undergo a dynamic kinetic resolution as R-3 could be converted to S-3 via the opening of a pyrrolidine ring (a retro aza-Michael/aza-Michael reaction) (Figure 2a).^{10,19} Alternatively, spontaneous decarboxylation of unreacted R-3 would lead to hygrine (**11**), which is also present in high concentrations in Erythroxylaceae plants.²⁰

With the determination of (+)-ecgonone (**7**) as an intermediate in cocaine biosynthesis, we sought to substantiate the overall pathway (Figures 1 and 2a). For example, we could not exclude the possibility that the downstream enzyme MecgoR would preferentially reduce (+)-**7** rather than (+)-**5** in *E. novogranatense* (Figure S13a).¹⁴ This is plausible due to their structural similarity (differing only in a methyl group), and also the instability of (+)-**7** has previously precluded its use as a substrate for MecgoR.¹⁴ To test this, both (+)-**5** and (+)-**7** were individually incubated with *EnMecgoR*. Conspicuously, only (+)-methylecgonone (**5**) could be efficiently reduced to form methylecgonine (**8**) (Figure S13), suggesting that the reduction process occurs after methylation by *EnMT4*.

De Novo Reconstruction of Cocaine in *N. benthamiana*. Although the biosynthesis of *N*-methyl- Δ^1 -pyrrolinium (**10**) in *E. novogranatense* was unknown, we designed to produce **10** in tobacco (*N. benthamiana*) using three known functional proteins (*EnODC*,²¹ *AbPMT1*²² from *Atropa belladonna*, and *NtMPO1*²³ from *N. tabacum*) (Figure 3a) as the same precursor **10** is implicated in the biosynthesis of cocaine (**1**), hyoscyamine (**2**), and nicotine.^{9,24} We also expressed five downstream cocaine biosynthesis-related proteins (*EnPKS1*,¹⁶ *EnCYP81AN15*, *EnMT4*, *EnMecgoR*,¹⁴

and *EnCS*¹⁵), as well as a benzoyl-CoA biosynthesis-related protein (*Aa4HBCL*:²⁵ benzoic acid CoA ligase from *Anthoceros agrestis*). This yielded 797.4 ± 19.5 ng cocaine (**1**) per milligram of dry plant weight with the supplement of benzoic acid (Figure 3b,c). When the substrate, benzoic acid, was removed (thereby relying on tobacco endogenous benzoic acid), the production of cocaine (**1**) was 398.3 ± 132.0 ng per milligram of dry plant weight. Subsequently, a similar yield of cocaine (259.5 ± 107.9 ng **1** per milligram of dry plant weight) was detected when *EnPKS1* was replaced by isozyme *AaPYKS1* from *Anisodus acutangulus*.

The essential nature of each engineered gene in tobacco was confirmed by gene dropout experiments (Figure 3d). As expected, the deletion of *AbPMT1*, *EnPKS1*, *EnCYP81AN15*, *EnMT4*, *EnMecgoR*, or *EnCS* led to the failure of cocaine production, with the lack of *EnMecgoR* leading to the accumulation of methylecgonone (**5**) and tropinone (**6**). On the other hand, the deletion of *EnMT4* resulted in the accumulation of tropinone (**6**). With the expression of six essential genes (*AbPMT1*, *EnPKS1* or *AaPYKS1*, *EnCYP81AN15*, *EnMT4*, *EnMecgoR*, and *EnCS*) in tobacco, the production of cocaine (**1**) was 60.5 ± 3.8 (*EnPKS1*) or 57.5 ± 20.3 (*AaPYKS1*) ng per milligram of dry plant weight, respectively.

DISCUSSION

Given their isolation in 1860 and 1831, respectively, it is unsurprising that cocaine (**1**) and hyoscyamine (**2**) possess such significant historical and contemporary importance. After more than 100 years of exploration, the biosynthetic route of hyoscyamine (**2**) was recently clarified, and its de novo reconstruction was realized in yeast.⁴ On the other hand, the biosynthesis of cocaine (**1**), and especially the genes responsible for the formation of the tropane skeleton, are still unknown. This can be attributed to the long-standing misapprehension of **4** as the biosynthetic intermediary, as well as the difficulties in synthesizing and detecting the true intermediate ecgonone (**7**). To decipher the biosynthetic route of the tropane skeleton in cocaine, we obtained an authentic standard of **7** utilizing the landmark tropinone synthesis of Robinson.¹⁷ By combining in vitro and in vivo enzyme activity assays, we identified that *EnCYP81AN15* and *EnMT4* are responsible for the formation of optical methylecgonone (**5**) from racemic **3**, notably via unstable **7**. At the same time, the biosynthesis of tropinone (**6**) in hyoscyamine should be detailed as follows: CYP82M3 actually catalyzes **3** to form **7**, which spontaneously decarboxylates to produce **6**. The isolation of **7** from Robinson's one-pot chemical reaction and subsequent detection in *EnCYP81AN15*- and CYP82M3-catalyzed reactions further illustrate the beauty of this biosynthetic approach.^{6,17,26}

Previously, virus-induced gene silencing (VIGS)¹¹ and isotopically labeled precursor feeding studies⁸ have indicated that MPOA (**3**) is a physiological substrate for tropinone (**6**) formation in the hyoscyamine (**2**) biosynthetic pathway. Although incorporation of MMPO (**4**) into cocaine (**1**) was observed in *E. coca*,⁷ transcriptome-based differential gene expression profiling and in vitro enzyme activity assay failed to identify enzymes catalyzing the formation of **4** and methylecgonone (**5**) from **3** and **4**, respectively. It is therefore reasonable to assume that, as seen in vitro, the labeled MMPO (**4**) was probably hydrolyzed to MPOA (**3**) in vivo prior to its incorporation into cocaine (**1**). As a result, a revised

biosynthetic module was successfully established, in which *EnCYP81AN15* and *EnMT4* catalyze the formation of optical methylecgonone (**5**) from racemic **3** via unstable **7**. Quite interestingly, two PKSs (*EnPKS1/2*) involved in the generation of **3** in *E. novogranatense* have recently been characterized,¹⁶ providing further evidence supporting a role of MPOA (**3**) as a physiological intermediate in the biosynthesis of cocaine. However, while *EnCYP81AN15* and *EnMT4* are strong candidates for catalyzing the tropane ring forming steps of cocaine biosynthesis, in the absence of in planta characterization, we cannot exclude the possibility that additional enzymes catalyze these reactions.

Despite the fact that the biosynthesis of intermediate *N*-methyl- Δ^1 -pyrrolinium (**10**) and benzoyl-CoA is still unknown in *E. novogranatense*, the well-known *PMT*²² and *MPO*²³ genes from hyoscyamine- or nicotine-producing plants and the widespread benzoyl-CoA biosynthetic genes^{27,28} could be used as substitutes. Utilizing tobacco endogenous benzoyl-CoA and genes, the de novo reconstruction of cocaine (**1**) was realized by the mini-combination of six genes in *N. benthamiana*. Further, this study prospectively enables the heterologous production of tropane alkaloids in microorganisms, which has far-reaching implications for pharmaceutical manufacture.

METHODS

Materials and Experimental Procedures. The reagents and solvents were purchased from standard commercial sources and used directly. All gene and fragment amplifications were carried out on a Bio-Rad T100 thermal cycler using Phanta Super Fidelity DNA Polymerase (Vazyme, China). PCR product purifications were performed using the FastPure Gel DNA Extraction Mini Kit (Vazyme, China). Plasmid purifications were performed using the FastPure Plasmid Mini Kit (Vazyme, China). 3-Oxo-glutaric acid was purchased from Sigma Aldrich Co. (USA).

Functional Verification of Candidate Genes in *N. benthamiana*. The *N. benthamiana* plants were grown in soil containing peat soil and vermiculite with a 16 h light cycle at room temperature. Plants were grown for 4–6 weeks before *Agrobacterium* infiltration.

The target pEAQ-HT plasmid was digested with *AgeI* and *XhoI* restriction enzymes (Thermo Scientific, USA) and was then assembled with the PCR products of candidate genes by using the ClonExpress Ultra One Step Cloning Kit (Vazyme, China). The assembly mixtures were transformed into chemically competent *E. coli* DH5 α . After selection by LB agar plates (10.0 g L⁻¹ peptone, 5.0 g L⁻¹ yeast extract, 10.0 g L⁻¹ NaCl, 15.0 g L⁻¹ agar, pH = 7.0–7.4) supplemented with kanamycin (50 μ g mL⁻¹) at 37 °C, positive constructs were verified by PCR and sequencing. Confirmed recombinant plasmids were transformed into *A. tumefaciens* LBA4404 using the freeze–thaw method. Transformants were selected on LB plates supplemented with rifampicin (20 μ g mL⁻¹), streptomycin (50 μ g mL⁻¹), and kanamycin (50 μ g mL⁻¹) at 30 °C. The obtained colonies were verified by PCR.

The positive colonies were grown on LB plates supplemented with rifampicin (20 μ g mL⁻¹), streptomycin (50 μ g mL⁻¹), and kanamycin (50 μ g mL⁻¹) at 30 °C. The cells were suspended in MMA buffer (10 mM MES, pH = 5.6, 10 mM MgCl₂, 150 μ M acetosyringone) to obtain *Agrobacterium* suspensions (OD₆₀₀ = 0.3 for each strain). The *Agrobacterium* suspensions were incubated at room temperature for 40 min and then infiltrated into *N. benthamiana* leaves using a 1 mL syringe. After 4 days, the corresponding substrate (see below) was infiltrated into previously *Agrobacterium*-infiltrated leaves. For the functional analysis of the SABATH methyltransferase candidate genes or the combined oxidase and methyltransferase genes, the injected substrate was 100 μ M deuterated MPOA (**3**). For the functional analysis of oxidase candidate genes, the injected substrate was 100 μ M

deuterated MMPO (4). Leaves were harvested 1 day later and were lyophilized to determine the dry weight of leaves.

Freeze-dried leaves from the previous step were ground in liquid nitrogen, directly extracted with CH_2Cl_2 . The organic layers were extracted with hydrochloric acid aqueous solution (pH = 2.0). Then, the pH of resulting aqueous layers was adjusted to 9.0 (1 M NaOH) and re-extracted with CH_2Cl_2 . The obtained organic layers were evaporated in vacuo and dissolved in acetonitrile. Exposure to methanol was avoided in the process of alkaloid extraction, as it could promote unintended esterification of 3 to form trace 4, thereby resulting in false-positive verification of the candidate methyltransferase.

The acetonitrile solutions were used for LC–MS analysis. The analysis was performed on a YMC-Triart C_{18} column (I.D. 4.6 mm \times 250 mm) using water with 0.1% formic acid (solvent A) and acetonitrile (solvent B). The injections were eluted with 10% B for 10 min, with a flow rate of 1.0 mL/min, with MS data collected in a positive ion mode (mass range: 50–400 m/z).

Expression and Purification of Candidate Proteins in *E. coli*.

The pET28a plasmid was digested with *Nde*I and *Bam*HI restriction enzymes. The PCR products of *EnMT2*, *EnMT4*, or *EnMecgoR* were assembled with a linearized pET28a plasmid. The assembly mixtures were transformed into chemically competent *E. coli* DH5 α . After selection by LB agar plates supplemented with kanamycin (50 $\mu\text{g mL}^{-1}$) at 37 °C, positive constructs were verified by PCR and sequencing. The positive recombinant plasmids were transformed into chemically competent *E. coli* BL21 (DE3), which were then plated for selection on LB agar with kanamycin (50 $\mu\text{g mL}^{-1}$). The positive transformants were verified by PCR.

The positive colonies of *EnMT2*-pET28a, *EnMT4*-pET28a, and *EnMecgoR*-pET28a were inoculated into LB liquid medium supplemented with kanamycin (50 $\mu\text{g mL}^{-1}$) and grown for 16 h at 37 °C. The overnight cultures were inoculated into 2 L of LB liquid medium supplemented with kanamycin (50 $\mu\text{g mL}^{-1}$) at 37 °C with shaking at 200 rpm to an OD₆₀₀ value of 0.6–0.8. The cultures were then cooled to 16 °C and induced by 0.2 mM isopropyl β -D-thiogalactoside (IPTG), before being further incubated at 16 °C for 18 h. The cell pellets were collected and resuspended in 50 mL of buffer A (20 mM imidazole, 50 mM Tris–HCl, 300 mM NaCl, 10% glycerol, pH = 8.0). All subsequent manipulations were performed at 4 °C. The suspensions were lysed by sonication. After centrifugation at 24,000 rpm for 30 min, the supernatants were loaded onto a HisTrap FF 5 mL column. The targeted protein fractions were obtained by the following elution method: (0–12.5 min, 100% buffer A; 12.5–25 min, 50% buffer A; 25–30 min, 100% buffer B; 30–37.5 min, 100% buffer A. buffer B: 500 mM imidazole, 50 mM Tris–HCl, 300 mM NaCl, 10% glycerol, pH = 8.0). The targeted protein fractions were concentrated by Amicon Ultra-4 centrifugal filters (Ultracel, 10,000 NMWL) at 4000 rpm. The obtained proteins were finally dissolved in 200 μL of storage buffer (100 mM $\text{NaH}_2\text{PO}_4/\text{Na}_2\text{HPO}_4$, 10% glycerol, pH = 7.0). The protein contents were estimated by measuring UV absorbance at 280 nm on a NanoDrop 2000c spectrophotometer (Thermo Scientific, USA).

In Vitro Characterization of *EnMT2* and *EnMT4* with Substrate 3. The assay mixtures (200 μL) which contained potassium phosphate buffer (50 mM $\text{K}_2\text{HPO}_4/\text{KH}_2\text{PO}_4$, pH 7.1), 1 mM SAM, 1 mM substrate 3, and 300 ng μL^{-1} *EnMT2* or *EnMT4* were incubated at 26 °C for 1 h. Assay which lacked enzyme served as a negative control (CK). The reactions were stopped by adding 2 μL of 1 M NaOH, before being extracted with 300 μL of CH_2Cl_2 . After the organic phase was evaporated, the reaction products were dissolved in 150 μL of acetonitrile and analyzed by LC–MS. The analysis was performed on a YMC-Triart C_{18} column (I.D. 4.6 mm \times 250 mm) using water with 0.1% formic acid (solvent A) and acetonitrile (solvent B). The injections were eluted with 10% B for 10 min, with a flow rate of 1.0 mL/min. The MS data were collected in a positive ion mode (mass range: 50–400 m/z).

Heterologous Expression of ESs and Isolation of Yeast Microsomes. The codon-optimized genes *EnCYP81AN15*sp or *DsCYP82M3*sp were inserted into the *AtATR1*-pESC-URA plasmid

(URA3 for yeast selection). This plasmid allowed the expressions of *EnCYP81AN15* or *DsCYP82M3* under the control of the *GAL1* promoter and the expression of *AtATR1* under the control of the *GAL10* promoter. The recombinant plasmids were then transformed into chemically competent *S. cerevisiae* BY4742 using the lithium acetate technique.²⁹ The colonies were inoculated into 5 mL of SC-URA liquid medium and grown for 16 h at 30 °C. The overnight cultures were further inoculated into 500 mL of SC-URA-R liquid medium (6.7 g L^{-1} yeast nitrogen base without amino acids, 20.0 g L^{-1} raffinose, 1.2 g L^{-1} amino acid mix without uracil) and grown for 48 h at 30 °C. The cells were then centrifuged, resuspended in SC-URA-G liquid medium (6.7 g L^{-1} yeast nitrogen base without amino acids, 20.0 g L^{-1} galactose, 1.2 g L^{-1} amino acid mix without uracil), and induced for 24 h. Following this, the cells were collected and resuspended in TEK buffer (50 mM Tris–HCl, 1 mM EDTA, 100 mM KCl, pH = 7.4), centrifuged again, and resuspended in TES buffer (50 mM Tris–HCl, 1 mM EDTA, 600 mM sorbitol, 0.25 mM PMSF, pH = 7.4). The cell suspensions were then disrupted by a high-pressure homogenizer, before the lysed cells were centrifuged at 7500g for 20 min. Finally, the supernatants were ultracentrifuged at 85,000g for 3 h, and the obtained microsomes were resuspended in TEG buffer (50 mM Tris–HCl, 1 mM EDTA, 20% glycerol, pH = 7.4).

In Vitro Characterization of ESs and *EnMT4* with Substrate 3.

For the co-incubation of *EnCYP81AN15* (or *DsCYP82M3*) and *EnMT4* with 3, the assay mixtures (100 μL) which contained potassium phosphate buffer (50 mM $\text{K}_2\text{HPO}_4/\text{KH}_2\text{PO}_4$, pH 7.5), 1 mM NADPH, 1 mM SAM, 1 mM substrate 3, 10 μL of microsomal proteins, and 100 ng μL^{-1} *EnMT4* were incubated at 30 °C for 30 min. The reactions were stopped by adding 2 μL of 1 M NaOH and were extracted with 300 μL of CH_2Cl_2 . After the organic phase was evaporated, the reaction products were dissolved in 150 μL of acetonitrile and analyzed by LC–MS (conditions were consistent with the assay of *EnMT4* with substrate 3 in vitro).

For the incubation of *EnCYP81AN15* or *DsCYP82M3* with 3, the assay mixtures (100 μL) which contained potassium phosphate buffer (50 mM $\text{K}_2\text{HPO}_4/\text{KH}_2\text{PO}_4$, pH 7.5), 1 mM NADPH, 100 μM substrate 3, and 10 μL of microsomal proteins were incubated at 30 °C. *AtATR1* microsomal proteins served as a negative control. The reactions were stopped by adding 100 μL of acetonitrile. The microsomal proteins were removed by centrifugation at 12,000 rpm for 10 min, and the supernatants were analyzed by LC–MS (conditions were consistent with the assay of *EnMT4* with substrate 3 in vitro).

In Vitro Characterization of *EnMT4* with Substrate 7. For the determination of the *EnMT4* function, the assay mixtures (100 μL) which contained potassium phosphate buffer (50 mM $\text{K}_2\text{HPO}_4/\text{KH}_2\text{PO}_4$, pH 7.5), 1 mM SAM, 1 mM substrate 7, and 100 ng μL^{-1} *EnMT4* were incubated at 30 °C for 1 h. Assays lacking an enzyme served as a negative control. The reactions were stopped by adding 100 μL of acetonitrile and analyzed by LC–MS (conditions were consistent with the assay of *EnMT4* with substrate 3 in vitro).

For the reaction of *EnMT4* with (+)-7 or (–)-7, the assay mixtures (100 μL) which contained potassium phosphate buffer (50 mM $\text{K}_2\text{HPO}_4/\text{KH}_2\text{PO}_4$, pH 8.0), 1 mM SAM, 300 μM substrate (+)-7 or (–)-7, and 5 ng μL^{-1} *EnMT4* were incubated at 35 °C for 10 min. The reactions were stopped by adding 100 μL of acetonitrile and analyzed by LC–MS (conditions were consistent with the assay of *EnMT4* with substrate 3 in vitro).

Substrate Selectivity of *EnCYP81AN15* and *DsCYP82M3*. The assay mixtures (100 μL) which contained potassium phosphate buffer (50 mM $\text{K}_2\text{HPO}_4/\text{KH}_2\text{PO}_4$, pH 7.5), 1 mM NADPH, 1 mM SAM, 50 μM substrate 3, 10 μL of microsomal proteins, and 100 ng μL^{-1} *EnMT4* were incubated at 35 °C for 30 min. The reactions were stopped by adding 300 μL of acetonitrile and analyzed by LC–MS (conditions were consistent with the assay of *EnMT4* with substrate 3 in vitro).

Substrate Selectivity of *EnMecgoR*. The assay mixtures (100 μL) which contained potassium phosphate buffer (50 mM $\text{K}_2\text{HPO}_4/\text{KH}_2\text{PO}_4$, pH 7.5), 1 mM NADPH, 0.3 mM (+)-7 or (+)-5, 600 ng

μL^{-1} *EnMecgoR* (and 1 mM SAM, 600 ng μL^{-1} *EnMT4*) were incubated at 35 °C for 20 min. The reactions were stopped by adding 100 μL of acetonitrile and analyzed by LC–MS (conditions were consistent with the assay of *EnMT4* with substrate 3 in vitro).

De Novo Reconstruction of Cocaine in *N. benthamiana*. The *Agrobacterium* suspensions of *EnODC*, *AbPMT1*, *NtMPO1*, *EnPKS1* (or *AaPYKS1*), *EnCYP81AN15*, *AtATR1*, *EnMT4*, *EnMecgoR*, *EnCS*, and *Aa4HBCL* were infiltrated into *N. benthamiana* leaves using a 1 mL syringe. After 5 days (benzoic acid was infiltrated into leaves on the fourth day), the leaves were harvested and lyophilized to determine the dry weight. The extraction method was conducted as previously described (Methods section: functional Verification of Candidate Genes in *N. benthamiana*). LC–MS analysis was performed (YMC-Triart C₁₈ column, I.D. 4.6 mm \times 250 mm) using water with 0.1% formic acid (solvent A) and acetonitrile (solvent B). The injections were eluted with a 28 min gradient mobile phase program (0.0–20.0 min, 10% B to 100% B; 20.0–24.0 min, 100% B; 24.1–28.0 min, 10% B). The MS data were collected in a positive ion mode (mass range: 50–400 *m/z*).

■ ASSOCIATED CONTENT

SI Supporting Information

The Supporting Information is available free of charge at <https://pubs.acs.org/doi/10.1021/jacs.2c09091>.

Additional experimental details, methods, assays, expression patterns of genes, functional analysis of *EnMT1–4* with supplemented MPOA (3) in *N. benthamiana*, in vitro characterization, chemical synthesis, HR-ESI-MS spectra, analysis of candidate genes, primers used, SDS-PAGE analysis and isolation of authentic standards, and NMR spectra described in this study (PDF)

Accession Codes

The transcriptome data sets of six different tissues (bud, young leaf, old leaf, stem, flower, and root) of *E. novogranatense* were deposited in the National Center for Biotechnology Information (NCBI) with accession numbers SRR15399168 to SRR15399180. The GenBank accession numbers for *EnODC*, *EnMT4*, *EnCYP81AN15*, *EnMecgoR*, and *EnCS* are ON647437, ON647436, ON647440, ON647438, and ON647439, respectively. All data supporting this article are also available from the authors upon request.

■ AUTHOR INFORMATION

Corresponding Author

Sheng-Xiong Huang – State Key Laboratory of Phytochemistry and Plant Resources in West China, and CAS Center for Excellence in Molecular Plant Sciences, Kunming Institute of Botany, Chinese Academy of Sciences, Kunming 650201, China; orcid.org/0000-0002-3616-8556; Email: sxhuang@mail.kib.ac.cn

Authors

Yong-Jiang Wang – State Key Laboratory of Phytochemistry and Plant Resources in West China, and CAS Center for Excellence in Molecular Plant Sciences, Kunming Institute of Botany, Chinese Academy of Sciences, Kunming 650201, China; University of Chinese Academy of Sciences, Beijing 100049, China

Jian-Ping Huang – State Key Laboratory of Phytochemistry and Plant Resources in West China, and CAS Center for Excellence in Molecular Plant Sciences, Kunming Institute of Botany, Chinese Academy of Sciences, Kunming 650201, China; State Key Laboratory of Southwestern Chinese

Medicine Resources, Innovative Institute of Chinese Medicine and Pharmacy, Chengdu University of Traditional Chinese Medicine, Chengdu 611137, China

Tian Tian – State Key Laboratory of Phytochemistry and Plant Resources in West China, and CAS Center for Excellence in Molecular Plant Sciences, Kunming Institute of Botany, Chinese Academy of Sciences, Kunming 650201, China; University of Chinese Academy of Sciences, Beijing 100049, China

Yijun Yan – State Key Laboratory of Phytochemistry and Plant Resources in West China, and CAS Center for Excellence in Molecular Plant Sciences, Kunming Institute of Botany, Chinese Academy of Sciences, Kunming 650201, China

Yin Chen – State Key Laboratory of Phytochemistry and Plant Resources in West China, and CAS Center for Excellence in Molecular Plant Sciences, Kunming Institute of Botany, Chinese Academy of Sciences, Kunming 650201, China; University of Chinese Academy of Sciences, Beijing 100049, China

Jing Yang – State Key Laboratory of Phytochemistry and Plant Resources in West China, and CAS Center for Excellence in Molecular Plant Sciences, Kunming Institute of Botany, Chinese Academy of Sciences, Kunming 650201, China

Jianghua Chen – CAS Key Laboratory of Tropical Plant Resources and Sustainable Use, Xishuangbanna Tropical Botanical Garden, Chinese Academy of Sciences, Kunming 650223, China

Yu-Cheng Gu – Syngenta Jealott's Hill International Research Centre, Bracknell, Berkshire RG42 6EY, U.K.; orcid.org/0000-0002-6400-6167

Complete contact information is available at:

<https://pubs.acs.org/doi/10.1021/jacs.2c09091>

Author Contributions

*Y.-J.W., J.-P.H., and T.T. contributed equally to this work.

Notes

The authors declare no competing financial interest.

■ ACKNOWLEDGMENTS

This research was supported by the National Key R&D Program of China (2018YFA0900600), the National Natural Science Foundation of China (Nos. 82225043, U1902212, and 32000239), the Strategic Priority Research Program of the CAS (No. XDB27020205), the Key Research Program of Frontier Sciences of the CAS (No. QYZDB-SSW-SMC051), and Yunnan Provincial Science and Technology Department (Nos. 2019FJ007 and 2019ZF011-2).

■ REFERENCES

- (1) Dillehay, T. D.; Rossen, J.; Ugent, D.; et al. Early Holocene coca chewing in northern Peru. *Antiquity* **2010**, *84*, 939–953.
- (2) Altman, A. J.; Albert, D. M.; Fournier, G. A. Cocaine's use in ophthalmology: our 100-year heritage. *Surv. Ophthalmol.* **1985**, *29*, 300–306.
- (3) Carroll, F. I.; Lewin, A. H.; Boja, J. W.; et al. Cocaine receptor: biochemical characterization and structure-activity relationships of cocaine analogs at the dopamine transporter. *J. Med. Chem.* **1992**, *35*, 969–981.
- (4) Srinivasan, P.; Smolke, C. D. Biosynthesis of medicinal tropane alkaloids in yeast. *Nature* **2020**, *585*, 614–619.

- (5) Qiu, F.; Yan, Y.; Zeng, J.; et al. Biochemical and metabolic insights into hyoscyamine dehydrogenase. *ACS Catal.* **2021**, *11*, 2912–2924.
- (6) Huang, J.-P.; Wang, Y.-J.; Tian, T.; et al. Tropane alkaloid biosynthesis: a centennial review. *Nat. Prod. Rep.* **2021**, *38*, 1634–1658.
- (7) Leete, E.; Bjorklund, J. A.; Couladis, M. M.; et al. Late intermediates in the biosynthesis of cocaine: 4-(1-methyl-2-pyrrolidiny)-3-oxobutanoate and methyl ecgonine. *J. Am. Chem. Soc.* **1991**, *113*, 9286–9292.
- (8) Abraham, T. W.; Leete, E. New intermediate in the biosynthesis of the tropane alkaloids in *Datura innoxia*. *J. Am. Chem. Soc.* **1995**, *117*, 8100–8105.
- (9) Lichman, B. R. The scaffold-forming steps of plant alkaloid biosynthesis. *Nat. Prod. Rep.* **2021**, *38*, 103–129.
- (10) Jamieson, C. S.; Misa, J.; Tang, Y.; et al. Biosynthesis and synthetic biology of psychoactive natural products. *Chem. Soc. Rev.* **2021**, *50*, 6950–7008.
- (11) Bedewitz, M. A.; Jones, A. D.; D'Auria, J. C.; et al. Tropinone synthesis via an atypical polyketide synthase and P450-mediated cyclization. *Nat. Commun.* **2018**, *9*, 5281.
- (12) Qu, L.; Li, S.; Xing, S. Methylation of phytohormones by the SABATH methyltransferases. *Chin. Sci. Bull.* **2010**, *55*, 2211–2218.
- (13) Zhao, N.; Ferrer, J. L.; Moon, H. S.; et al. A SABATH methyltransferase from the moss *Physcomitrella Patens* catalyzes S-methylation of thiols and has a role in detoxification. *Phytochemistry* **2012**, *81*, 31–41.
- (14) Jirschitzka, J.; Schmidt, G. W.; Reichelt, M.; et al. Plant tropane alkaloid biosynthesis evolved independently in the Solanaceae and Erythroxylaceae. *Proc. Natl. Acad. Sci. U. S. A.* **2012**, *109*, 10304–10309.
- (15) Schmidt, G. W.; Jirschitzka, J.; Porta, T.; et al. The last step in cocaine biosynthesis is catalyzed by a BAHD acyltransferase. *Plant Physiol.* **2015**, *167*, 89–101.
- (16) Tian, T.; Wang, Y.-J.; Huang, J.-P.; et al. Catalytic innovation underlies independent recruitment of polyketide synthases in cocaine and hyoscyamine biosynthesis. *Nat. Commun.* **2022**, *13*, 4994.
- (17) Robinson, R. A synthesis of tropinone. *J. Chem. Soc.* **1917**, *111*, 762–768.
- (18) Findlay, S. P. Concerning 2-carbomethoxytropinone. *J. Org. Chem.* **1957**, *22*, 1385–1394.
- (19) Eich, E. Ornithine-derived alkaloids. In: *Solanaceae and convolvulaceae: secondary metabolites*; Springer-Verlag: Berlin Heidelberg, 2008; pp 33–212.
- (20) Johnson, E. L. Alkaloid content in *Erythroxylum coca* tissue during reproductive development. *Phytochemistry* **1996**, *42*, 35–38.
- (21) Docimo, T.; Reichelt, M.; Schneider, B.; et al. The first step in the biosynthesis of cocaine in *Erythroxylum coca*: the characterization of arginine and ornithine decarboxylases. *Plant Mol. Biol.* **2012**, *78*, 599–615.
- (22) Junker, A.; Fischer, J.; Sichhart, Y.; et al. Evolution of the key alkaloid enzyme putrescine N-methyltransferase from spermidine synthase. *Front. Plant Sci.* **2013**, *4*, 260.
- (23) Naconsie, M.; Kato, K.; Shoji, T.; et al. Molecular evolution of N-methylputrescine oxidase in tobacco. *Plant Cell Physiol.* **2014**, *55*, 436–444.
- (24) Kohnen-Johannsen, K. L.; Kayser, O. Tropane alkaloids: chemistry, pharmacology, biosynthesis and production. *Molecules* **2019**, *24*, 796.
- (25) Wohl, J.; Petersen, M. Phenolic metabolism in the hornwort *Anthoceros agrestis*: 4-coumarate CoA ligase and 4-hydroxybenzoate CoA ligase. *Plant Cell Rep.* **2020**, *39*, 1129–1141.
- (26) Huang, J.-P.; Fang, C.; Ma, X.; et al. Tropane alkaloids biosynthesis involves an unusual type III polyketide synthase and non-enzymatic condensation. *Nat. Commun.* **2019**, *10*, 4036.
- (27) Widhalm, J. R.; Dudareva, N. A familiar ring to it: biosynthesis of plant benzoic acids. *Mol. Plant* **2015**, *8*, 83–97.
- (28) Lackus, N. D.; Schmidt, A.; Gershenzon, J.; et al. A peroxisomal β -oxidative pathway contributes to the formation of C₆-C₁ aromatic volatiles in poplar. *Plant Physiol.* **2021**, *186*, 891–909.
- (29) Gietz, R. D.; Schiestl, R. H. Large-scale high-efficiency yeast transformation using the LiAc/SS carrier DNA/PEG method. *Nat. Protoc.* **2007**, *2*, 38–41.

Recommended by ACS

Intramolecular C–C Bond Formation Links Anthraquinone and Eneidyne Scaffolds in Tiansimycin Biosynthesis

Chun Gui, Ben Shen, et al.

OCTOBER 24, 2022
JOURNAL OF THE AMERICAN CHEMICAL SOCIETY

READ 

Characterization of a Radical SAM Oxygenase for the Ether Crosslinking in Darobactin Biosynthesis

Hai Nguyen, Kenichi Yokoyama, et al.

OCTOBER 04, 2022
JOURNAL OF THE AMERICAN CHEMICAL SOCIETY

READ 

Identification and Characterization of a Cryptic Bifunctional Type I Diterpene Synthase Involved in Talaronoid Biosynthesis from a Marine-Derived Fungus

Peng Zhang, Jaclyn M. Winter, et al.

SEPTEMBER 20, 2022
ORGANIC LETTERS

READ 

Depside Bond Formation by the Starter-Unit Acyltransferase Domain of a Fungal Polyketide Synthase

Lin Chen, Yudai Matsuda, et al.

OCTOBER 12, 2022
JOURNAL OF THE AMERICAN CHEMICAL SOCIETY

READ 

Get More Suggestions >